

Synthesis, Structure and Photophysical Properties of a Dinuclear Copper(I) Complex Based on Phosphino-pyridine and Diphosphine Mixed-ligands^①

YU Wen-Si HUANG Chun-Hua HUANG Xi-He^②

(Institute of Optical Crystalline Materials, College of Chemistry, Fuzhou University, Fuzhou 350116, China)

ABSTRACT Treatment of bis(diphenylphosphino)methane (dppm) and 2-(diphenylphosphanyl)pyridine (dpppy) with $\text{Cu}(\text{CH}_3\text{CN})_4\text{BF}_4$ afforded a dinuclear Cu(I) complex $[\text{Cu}_2(\text{dpppy})_2(\text{dppm})(\text{CH}_3\text{CN})](\text{BF}_4)_2 \cdot 3\text{CH}_2\text{Cl}_2$ (**1**). Complex **1** was structurally characterized by X-ray single-crystal analysis and its photophysical properties were studied in detail. It crystallizes in triclinic space group $P\bar{1}$ with $a = 13.0834(8)$, $b = 13.5568(8)$, $c = 21.8544(11)$ Å, $\alpha = 76.090(5)^\circ$, $\beta = 80.803(5)^\circ$, $\gamma = 64.582(6)^\circ$, $V = 3391.3(3)$ Å³, $Z = 2$, $M_r = 1507.42$, $D_c = 1.476$ g/cm³, $F(000) = 1532$, $\text{GOOF} = 1.071$, the final $R = 0.0700$ for 9041 observed reflections with $I > 2\sigma(I)$ and $wR = 0.2063$ for all data. The complex contains a Cu_2 -core structure surrounded by one dppm and two dpppy ligands in a head-to-head arrangement. In the crystalline phase, complex **1** exhibits bright bluish-green photoluminescence ($\lambda_{\text{max}} = 488$ nm) with high quantum yield ($\phi = 0.57$) at room temperature. It is still a relatively high emission quantum yield ($\phi = 0.36$) in doped PMMA thin film with 20 wt% dopant of complex **1**. The emission peaks of **1** in dichloromethane solution and doped PMMA (20 wt%) thin films are 510 and 494 nm, respectively, showing a very slight bathochromic shift compared to that in crystalline phase. This phenomenon might be attributed to its rigid conformation that precludes the possible distortion of copper centers in the excited state.

Keywords: copper(I) complex, thermally activated delayed fluorescence, crystalline structure;

DOI: 10.14102/j.cnki.0254-5861.2011-2788

1 INTRODUCTION

Luminescent organometallic complexes have attracted considerable current attention owing to their applications ranging from photocatalysis, chemo-, bio-sensing to dye-sensitized solar cells and organic electronics^[1-3]. For these applications, phosphorescent complexes of noble metals, especially Ir(III) and Pt(II), have been investigated extensively^[4, 5]. With strong spin orbital coupling (SOC), phosphorescent materials can harvest both singlet and triple excitons, resulting in a theoretically 100% internal quantum efficiency. However, these materials are highly expensive and their metal resources are very limited, and hence it is desired to find an alternative strategy based on less expensive and more abundant materials. Emissive copper(I) complexes represent a promising alternative candidate due to their rich structures, excellent photophysical properties, and abound in

natural resources^[6]. Although the small SOC effect of copper(I) complexes is not enough to promote efficient phosphorescence. However, this severe restriction can be overcome *via* an additional radiative decay channel, *i.e.* thermally activated delayed fluorescence (TADF). The singlet state can be thermally activated at the expense of the triplet state, when the energy separation $\Delta E(S_1 - T_1)$ between the lowest singlet (S_1) and triplet (T_1) excited states is small (< 3000 cm⁻¹). This allows the copper(I) complexes to harvest both singlet and triplet excitations, resulting in theoretically 100% internal quantum efficiency at ambient temperature. The emission decay time can also be drastically lowered as it comes up to noble metal emissions at ambient temperature^[7-10]. Up to date, copper(I) complexes with pronounced metal and/or ligand to ligand charge transfer ((M+L)LCT) character are the most studied metal-containing TADF materials^[7, 11, 12].

Received 26 February 2020; accepted 14 April 2020

① This work was supported by the Natural Science Foundation of Fujian Province (2017J01576)

② Corresponding author. E-mail: xhhuang@fzu.edu.cn

However, for a four-coordinate complex, most Cu(I)-based TADF material undergoes a typical geometry distortion on the Cu(I) center under excited state. Such flattening distortions usually result in a very effective non-radiative pathway owing to an increase of the Franck-Condon factors that couple the excited and ground states^[11]. The decrease of PLQY is especially distinct when the four-coordinate Cu(I) emitter is located on a non-rigid matrix, for example, a doped thin film. Thanks to the pioneering study of McMillin *et al.*^[13], a great number of heteroleptic Cu(I) complexes with various N-heterocyclic and/or phosphine ligands containing sterically hindered substitutes have been reported up to date^[9, 10]. These complexes showed an important increase in the structural rigidity and stability to block geometry distortion under excited state, and thus offer a significant improvement on the emission efficiencies. For example, Harkins and Peters reported a highly emissive bimetallic copper(I) complex, [Cu(PNP)]₂ (PNP = bis(2-diisobutylphosphinophenyl)amido), in which the two tetrahedral Cu(I) centers are bridged by the amido groups of rigid, bulky PNP ligand^[14]. Subsequently, they reported an analogous complex [Cu(PNP-^tBu)]₂ (PNP-^tBu = bis(2-diisobutylphosphino-4-*tert*-butyl phenyl)-amido), showing a high external quantum efficiency (EQE) of 16.1%^[8]. Yersin *et al.* reported three Cu(I) complexes built from a tri-dentate tris(2-pyridyl)methane and three monodentate phosphine ligands, namely, triphenylphosphine, tris(ortho-tolyl)phosphine and tris(ortho-*n*-butylphenyl)phosphine^[15]. Owing to the giant sterical substituents, the latter shows a high emission quantum yield even in a dichloromethane solution ($\Phi_{\text{PL}} = 76\%$) than the former ($\Phi_{\text{PL}} \ll 1\%$).

In this paper, we present a new heteroleptic Cu(I) complex with a rigid dinuclear structure, namely [Cu₂(dpppy)₂(dppm)-(CH₃CN)](BF₄)₂ 3CH₂Cl₂ (**1**). The complex exhibits bluish-green photoluminescence ($\lambda_{\text{max}} = 488$ nm) with high quantum yield ($\phi = 0.57$) in crystalline phase at room temperature. It is still a relatively high emission quantum yield ($\phi = 0.36$) in doped PMMA thin film with 20 wt% dopant of complex **1**. Interestingly, the emission peaks of **1** in solution and the doped PMMA thin film are 494 and 510 nm, respectively, showing a very slight bathochromic shift compared to that in crystalline phase. The synthesis, structure and photophysical investigation are carried out.

2 EXPERIMENTAL

2.1 Materials and instruments

All commercially available reagents were used as received without any purification. Solvents were freshly distilled over appropriate drying reagents. All manipulations were conducted in air. The complex [Cu(CH₃CN)₄]BF₄ was prepared using the literature procedure^[16]. Elemental analyses of C, H and N were carried out with a Vario EL III elemental analyzer. FT-IR spectra were recorded from KBr pellets in the range of 4000~400 cm⁻¹ on a Thermo Fisher Nicolet IS50 FT-IR spectrometer. UV-Vis absorption spectra were obtained on a Perkin-Elmer lambda 900 UV-Vis spectrometer. UV-Vis solid diffuse reflection spectra were measured on a Varian CARY 500 UV-Vis-NIR spectrometer. Luminescence spectra and lifetime measurements were carried out on an Edinburgh Instrument F920 fluorescent spectrometer. The luminescence quantum yields were recorded on a Hamamatsu Photonics C11347-11 absolute photoluminescence quantum yield spectrometer.

2.2 Synthesis of [Cu₂(dpppy)₂(dppm)(CH₃CN)]-(BF₄)₂ 3CH₂Cl₂ (**1**)

A mixture of [Cu(CH₃CN)₄]BF₄ (15.7 mg, 0.05 mmol), bis(diphenylphosphino)methane (dppm, 19.2 mg, 0.05 mmol) and 2-(diphenylphosphanyl)pyridine (dpppy, 13.1mg, 0.05 mmol) in 5.0 mL CH₃CN and 5.0 mL CH₂Cl₂ was stirred for 8 h and then filtering. After slow diffusion of diethyl ether vapour to the filtrate at room temperature, colorless block single crystals of **1** suitable for X-ray diffraction measurements were obtained after 3 days. Yield: 25.6 mg (68% based on Cu). Anal. Calcd. for C₆₄H₅₉N₃P₄Cu₂B₂Cl₆F₈: C, 51.00; H, 3.95; N, 2.79. Found: C, 50.89; H, 3.79; N, 2.90. IR (KBr pellet, cm⁻¹): 3058(w), 1583(w), 1482(w), 1433(m), 1095(s), 740(s), 692(s), 506(s), 414(m).

2.3 Single-crystal structure analysis

Suitable single crystal of complex **1** with approximate dimensions of 0.42mm × 0.29mm × 0.23mm was mounted on glass fibers for X-ray measurement. Reflection data were collected at 173(2) K on a Rigaku Saturn724 CCD diffractometer with graphite-monochromatized MoK α radiation ($\lambda = 0.71073$ Å). The data set was corrected for Lorentz and Polarization factors as well as for absorption by a multi-scan method. The structure was solved by direct methods and refined by full-matrix least-squares on F^2 using the SHELX-97 program^[17, 18]. All non-hydrogen atoms were refined with anisotropic thermal parameters. Hydrogen atoms were located at the geometrical positions and refined with isotropical thermal parameters. A total of 24649 reflections were obtained in the range of 2.31< θ <25.03° with 11524 unique

ones ($R_{\text{int}} = 0.0407$). The final $R = 0.0700$ for 9041 observed reflections with $I > 2\sigma(I)$ and $wR = 0.2063$ for all data, and

$GOOF = 1.071$. Some selected bond lengths and bond angles are summarized in Table 1.

Table 1. Selected Bond Lengths (Å) and Angles (°) of Complex 1

Bond	Dist.	Bond	Dist.
Cu(1)–P(1)	2.3172(15)	Cu(1)–P(3)	2.3122(14)
Cu(1)–P(4)	2.3057(15)	Cu(1)–N(3)	2.027(5)
Cu(2)–P(2)	2.2044(15)	Cu(2)–N(1)	2.031(5)
Cu(2)–N(2)	2.034(5)	Cu(1)··Cu(2)	2.8739(9)
Angle	(°)	Angle	(°)
P(1)–Cu(1)–P(3)	114.03(5)	P(1)–Cu(1)–P(4)	123.26(5)
P(3)–Cu(1)–P(4)	111.99(5)	P(1)–Cu(1)–N(3)	102.21(14)
P(3)–Cu(1)–N(3)	98.93(14)	P(4)–Cu(1)–N(3)	101.58(14)
P(2)–Cu(2)–N(1)	127.58(13)	P(2)–Cu(2)–N(2)	124.09(14)
N(1)–Cu(2)–N(2)	103.10(19)		

3 RESULTS AND DISCUSSION

3.1 Crystal structures

Complex **1** was prepared from the reaction of $\text{Cu}(\text{CH}_3\text{CN})_4\text{BF}_4$, dpppy and slightly excessive dppm ligand by a diffusion procedure. The formation of complex **1** was identified by elemental analysis and FTIR spectroscopy. In the FTIR spectrum of **1**, the peaks at 1583, 1482 and 1433 cm^{-1} show the asymmetric and symmetric stretching of the pyridine and phenyl rings. Single-crystal X-ray diffraction study reveals complex **1** crystallizes in triclinic space group $P\bar{1}$. The structure of **1** consists of cationic Cu(I)-dinuclear structure and anionic boron tetrafluoride, acetonitrile as coordinated molecule and dichloromethane as interstitial molecules. The cationic binuclear structure of Cu(I) complex contains a Cu_2 -core surrounded by three ligands, namely one dppm and two dpppy ligands in a head-to-head arrangement, as well as one acetonitrile as coordinated molecule. As shown in Fig. 1, two Cu(I) centers are in three- and four-coordinated

geometries, respectively. The Cu(2) atom forms a slightly distorted trigonal coordination geometry with one P atom of dppm ligand and two pyridine groups from two dpppy ligands. The sum of bonded angles involving the Cu(2) center of 354.77° is very close to 360° , implying an approaching planar trigonal coordination geometry. The Cu(1) atom is in a distorted tetrahedral configuration with three P atoms from one dppm and two dpppy ligands and an additional N atom from an acetonitrile molecule. The P–Cu–P and P–Cu–N bond angles range from $98.93(14)$ to $123.26(5)^\circ$. The Cu··Cu separation of $2.8739(9)$ Å is slightly larger than the sum of *van der Waals* radius of Cu (about 2.8 Å), thus too long to qualify as a cuprophilic interaction. All the bond distances and bond angles are similar to the reported complex prepared from dpppy or dppm^[19]. The Cu–P bond length for Cu(2) ($2.2044(15)$ Å) is slightly shorter than for Cu(1) ($2.3057(15)$ – $2.3172(15)$ Å), however, there is not obvious difference between the Cu–N bond lengths for Cu(1) and Cu(2) atoms.

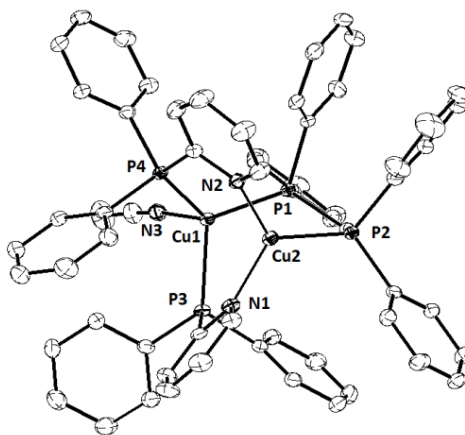


Fig. 1. X-ray structure of the cationic Cu(I)-dinuclear structure of **1** with probability ellipsoids set to 30%

3.2 Photophysical properties

The absorption spectra of complex **1**, dpppy and dppm ligands are shown in Fig. 2a. All spectra were recorded under ambient conditions for the complex and free ligands dissolved in dichloromethane ($c \approx 1.0 \times 10^{-5} \text{ mol L}^{-1}$). Both of the free dpppy and dppm ligands display strong absorption peaks at 227 and 230 nm, and broad absorption peaks around 258 and 270 nm, respectively. The electronic transitions of the two free ligands can be assigned to the ligand-centered (LC) $\pi \rightarrow \pi^*$ and/or $n \rightarrow \pi^*$ transitions of phosphine and N-heterocyclic groups. Complex **1** also exhibits a strong absorption peak at 232 nm and a broad absorption band within about 240~300 nm wavelength region as a shoulder

peak. Such corresponding electronic transitions can be attributed definitely similar to the two free ligands. Additionally, at longer wavelengths over 300~370 nm, distinctly weaker absorption bands are observed from complex **1**, which did not appear for free ligands. This absorption band can be attributed to metal-to-ligand charge transfer (MLCT) transitions^[7, 20]. The solid state UV-Vis diffuse reflectance spectrum of **1** was measured at room temperature and the absorption data are calculated from the reflectance using the Kubelka-Munk function $\alpha/S = (1 - R)^2/(2R)$ (Fig. 2b)^[20]. The complex exhibits a broad band with absorption edge at 3.20 eV (388 nm), which can further confirm the presence of MLCT transitions.

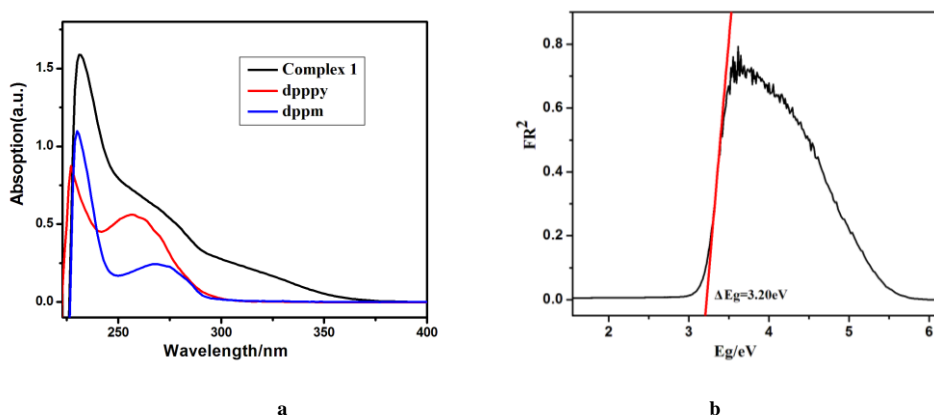


Fig. 2. a) Absorption spectra of **1** together with free dpppy and dppm ligands recorded in dichloromethane solution, and b) Solid state UV-Vis diffuse reflectance spectrum of **1** measured at room temperature

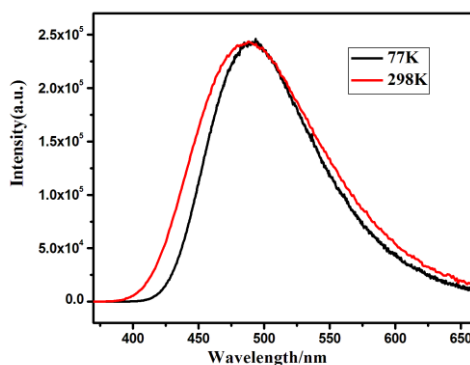


Fig. 3. Luminescence spectra of complex **1** in the solid state ($\lambda_{\text{ex}} = 365 \text{ nm}$) at 298 and 77 K

Fig. 3 displays the emission spectra of complex **1** measured at $T = 298$ and 77 K in the solid state. The selected data of the emissive properties are listed in Table 3. The spectra are broad and featureless, indicating that the emission originates from a charge-transfer transition which, in this case, has significant metal-to-ligand charge transfer (MLCT) character. At 298 K, complex **1** exhibits strong bluish green photoluminescence with a high PLQY ($\Phi = 57.3\%$) and an

emissive maximum at 488 nm under excitation with UV light (365 nm) in the solid state. The emission lifetime is $\tau = 25.9 \mu\text{s}$. The radiative rate constants ($k_r = \Phi\tau^{-1}$) at 298 K can be determined to be $2.2 \times 10^4 \text{ s}^{-1}$. Upon cooling from 298 to 77 K under an excitation at 365 nm, a red shift of the emission maximum from 488 to 493 nm is observed and the emission lifetime increases by about 5 times to 130.1 μs . This phenomenon suggests that the photoluminescence of complex

1 may be assigned to TADF at room temperature. At 77 K, the predominant population is the triplet state and thus the emitting state can be assigned as pure T_1 state. With temperature increase, gradually thermal population of the upper lying S_1 state occurs *via* efficient up-conversion from the T_1 state, and the emissions of **1** mainly originate from the

S_1 state at room temperature^[21]. The energy separation between the S_1 and T_1 states of $\Delta E(S_1 - T_1) = 810 \text{ cm}^{-1}$ can roughly evaluate from the onsets of emission spectra at 77 and 298 K. The value falls in the range of $\Delta E(S_1 - T_1)$ energy separation ($< 3000 \text{ cm}^{-1}$), which is typical for TADF material^[9].

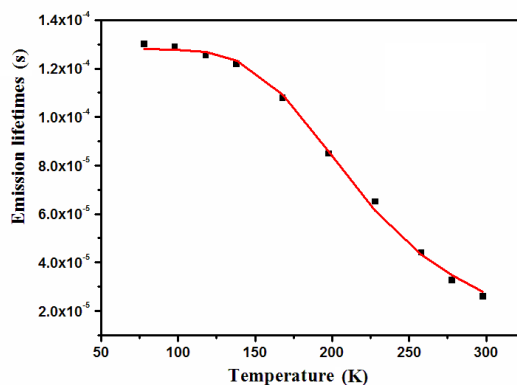


Fig. 4. Emission lifetime of complex **1** in solid state versus temperature

To clarify the emission properties further, the temperature dependence of the emission lifetimes of complex **1** was investigated. As shown in Fig. 4, the lifetime of complex **1** changed gradually from 77 to 140 K, and then a sharp decrease in the lifetime was observed at higher temperature above 140 K. Under the assumption of a fast thermal equilibrium between the S_1 and T_1 states, the observed decay time (τ_{obs}) can be given as a Boltzmann average by using the equation as follows^[9]:

$$\tau_{\text{obs}} = \frac{3 + \exp(-\Delta E/RT)}{\frac{3}{\tau_{T_1}} + \frac{1}{\tau_{S_1}} \exp(-\Delta E/RT)} \quad (\text{Eq. 1})$$

Herein, R and T are the ideal gas constant and absolute temperature, respectively. τ_{S_1} and τ_{T_1} are the individual emission lifetime of S_1 and T_1 states, and ΔE is the energy separation between the two states, i.e. the $\Delta E(S_1 - T_1)$ as men-

tioned above. The values of τ_{S_1} , τ_{T_1} and $\Delta E(S_1 - T_1)$ are determined from this equation and listed in Table 2. The fitted τ_{T_1} values approximate to the values observed at 77 K, and the $\Delta E(S_1 - T_1)$ values agree well with the energy difference between the onsets of emission spectra at 77 and 298 K. The small $\Delta E(S_1 - T_1)$ values observed from complex **1** can be rationalized by an effective spatial separation between the frontier orbitals, which results in a small exchange energy and thus a small singlet-triplet splitting. The small singlet-triplet energy splitting is beneficial to an efficient thermally activated up intersystem crossing and result in a dominant TADF emission at high temperature. It is noteworthy that the lower overlap between the HOMO and LUMO can also result in a decrease of the radiative rate of $S_1 \rightarrow S_0$ transition, generating a longer singlet state decay lifetime (larger τ_{S_1} value)^[22].

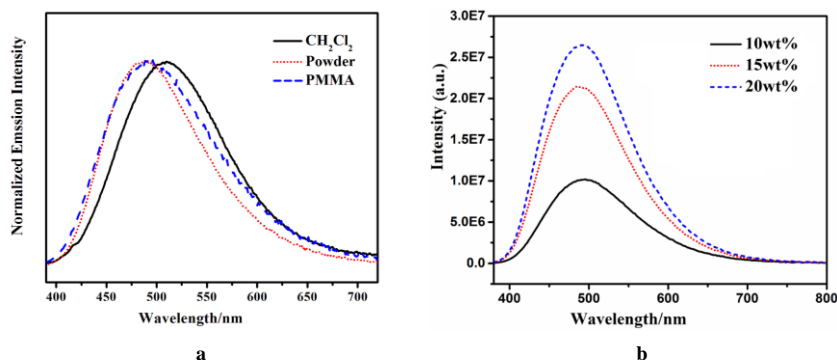


Fig. 5. a) Luminescence spectra of **1** measured in powder, doping PMMA thin film (20 wt%), and CH_2Cl_2 solution, and b) measured in PMMA thin film with different doped weight ($\lambda_{\text{ex}} = 365 \text{ nm}$) at room temperature

Table 2. Emission Properties of **1** in the Solid State at 298 and 77 K, and the Fitting Parameters Based on Eq. (1)

Emission properties		Fitting parameters	
λ_{\max} (298 K) (nm)	488	$\Delta E(S_1 - T_1)$ (cm ⁻¹ /eV)	812/0.10
τ (298 K) (μ s)	25.9	τ_{T1} (μ s)	130
Φ_{PL} (298K) (%)	57.3	τ_{S1} (ns)	232
λ_{\max} (77 K) (nm)	493		
τ (77 K) (μ s)	130.1		

Table 3. Emission Properties of **1** in Different Environments at Ambient Temperature

	λ_{\max} (nm)	Φ_{PL} (%)
Powders	488	57.3
PMMA (10wt%) ^a	492	27.2
PMMA (15wt%) ^a	494	33.4
PMMA (20wt%) ^a	494	36.1
CH ₂ Cl ₂ ^b	510	1.2

a) Dopant concentrations in PMMA matrices are 10%, 15% and 20% weight, respectively

b) The concentration in CH₂Cl₂ solution is 1.0×10^{-5} mol/L

In order to examine the influence of different environments on the photoluminescence, ambient temperature emission spectra of complex **1** were investigated in powder, complex doping PMMA thin films, and dichloromethane solution, respectively (Fig. 5). The corresponding emission maxima as well as the corresponding quantum yields are summarized in Table 3 for **1** measured in powder, PMMA thin films, and solution, respectively. The emission maxima for **1** investigated as powder are shifted to longer wavelengths when measured in PMMA thin films and solution. It is noteworthy that only very slight red-shifts were observed for different dopant concentrations in PMMA matrices, exhibiting emission maxima in the range of 492~494 nm. The observed red shift is somewhat larger when measured in solution with maxima of 510 nm. In spite of this, the red-shift values are still far less than many reported Cu(I) analogues both in solution and PMMA thin films. The phenomenon is definitely attributed to a rigid conformation that precludes the possible distortion of the copper centers in excited state^[23]. The emission quantum yield drops considerably, when measured in powder with ϕ_{PL} values of 57.3%, to dichloromethane

solutions with only 1.2%. However, the values of PMMA matrices with different ratios lie between 27.1% and 36.1%, slightly lower than that measured in powder.

4 CONCLUSION

In summary, we prepared a new dinuclear Cu(I) complex based on bis(diphenylphosphino)-methane and 2-(diphenylphosphanyl)-pyridine ligands. The complex shows strong bluish-green photoluminescence with high quantum yield ($\phi = 0.57$) at room temperature, for which the crystal structure and emission nature have been identified by X-ray diffraction structure analysis and photophysical studies. These is still a relatively higher emission quantum yield ($\phi = 0.36$) in doped PMMA thin film with 20 wt% dopant of complex **1**. Furthermore, the emission peaks of the title complex in solution and doped PMMA thin films exhibit very slight bathochromic shifts compared to that in crystalline phase. This phenomenon can be attributed to its rigid conformation that precludes the possible distortion of the copper in the excited state.

REFERENCES

- (1) Uoyama, H.; Goushi, K.; Shizu, K.; Nomura, H.; Adachi, C. Highly efficient organic light-emitting diodes from delayed fluorescence. *Nature* **2012**, 492, 234–238.
- (2) Bizzarri, C.; Spuling, E.; Knoll, D. M.; Volz, D.; Bräse, S. Sustainable metal complexes for organic light-emitting diodes (OLEDs). *Coord. Chem. Rev.* **2018**, 373, 49–82.
- (3) Yang, M.; Chen, X. L.; Lu, C. Z. Efficiently luminescent copper(I) iodide complexes with crystallization-induced emission enhancement (CIEE). *Dalton Trans.* **2019**, 48, 10790–10794.
- (4) Fleetham, T.; Li, G.; Li, J. Phosphorescent Pt(II) and Pd(II) complexes for efficient, high-color-quality, and stable OLEDs. *Adv. Mater.* **2017**, 29,

1601861.

- (5) Wu, Y.; Tan, X.; Lv, A.; Yu, F.; Ma, H.; Shen, K.; Sun, Z.; Chen, F.; Chen, Z. K.; Hang, X. C. Triplet excited-state engineering of phosphorescent Pt(II) complexes. *J. Phys. Chem. Lett.* **2019**, 10, 5105–5110.
- (6) Femoni, C.; Muzzioli, S.; Palazzi, A.; Stagni, S.; Zacchini, S.; Monti, F.; Accorsi, G.; Bolognesi, M.; Armaroli, N.; Massi, M.; Valenti, G.; Marcaccio, M. New tetrazole-based Cu(I) homo- and hetero-leptic complexes with various P[^]P ligands: synthesis, characterization, redox and photophysical properties. *Dalton Trans.* **2013**, 42, 997–1010.
- (7) Yersin, H.; Rausch, A. F.; Czerwieniec, R.; Hofbeck, T.; Fischer, T. The triplet state of organo-transition metal compounds. Triplet harvesting and singlet harvesting for efficient OLEDs. *Coord. Chem. Rev.* **2011**, 255, 2622–2652.
- (8) Deaton, J. C.; Switalski, S. C.; Kondakow, D. Y.; Young, R. H.; Pawlik, T. D.; Giesen, D. J.; Harkins, S. B.; Miller, A. J. M.; Mickenberg, S. F.; Peters, J. C. E-Type delayed fluorescence of a phosphine-supported Cu₂(μ-NAr₂)₂ diamond core: harvesting singlet and triplet excitons in OLEDs. *J. Am. Chem. Soc.* **2010**, 132, 9499–9508.
- (9) Hofbeck, T.; Monkowius, U.; Yersin, H. Highly efficient luminescence of Cu(I) compounds: thermally activated delayed fluorescence combined with short-lived phosphorescence. *J. Am. Chem. Soc.* **2015**, 137, 399–404.
- (10) Czerwieniec, R.; Leidl, M. J.; Homeier, H. H. H.; Yersin, H. Cu(I) complexes-thermally activated delayed fluorescence. photophysical approach and material design. *Coord. Chem. Rev.* **2016**, 325, 2–28.
- (11) Mara, M. W.; Fransted, K. A.; Chen, L. X. Interplays of excited state structures and dynamics in copper(I) diimine complexes: implications and perspectives. *Coord. Chem. Rev.* **2015**, 282, 2–18.
- (12) Jia, J. H.; Chen, X. L.; Liao, J. Z.; Liang, D.; Yang, M. X.; Yu, R.; Lu, C. Z. Highly luminescent copper(I) halide complexes chelated with a tetradentate ligand (PNNP): synthesis, structure, photophysical properties and theoretical studies. *Dalton Trans.* **2019**, 48, 1418–1426.
- (13) Cuttell, D. G.; Kuang, S. M.; Fanwick, P. E.; McMillin, D. R.; Walton, R. A. Simple Cu(I) complexes with unprecedented excited-state lifetimes. *J. Am. Chem. Soc.* **2002**, 124, 6–7.
- (14) Harkins, S. B.; Peters, J. C. A highly emissive Cu₂N₂ diamond core complex supported by a [PNP]-ligand. *J. Am. Chem. Soc.* **2005**, 127, 2030–2031.
- (15) Schinabeck, A.; Rau, N.; Klein, M.; Sundermeyer, J.; Yersin, H. Deep blue emitting Cu(I) tripod complexes. Design of high quantum yield materials showing TADF-assisted phosphorescence. *Dalton Trans.* **2018**, 47, 17067–17076.
- (16) Kubas, G. J. *Inorg. Synth.* **1990**, 26, 68.
- (17) Sheldrick, G. M. *SHELXS-97, Program for Crystal Structure Solution*. University of Göttingen, Germany **1997**.
- (18) Sheldrick, G. M. *SHELXL-97, Program for Crystal Structure Refinement*. University of Göttingen, Germany **1997**.
- (19) Kang, L.; Chen, J.; Teng, T.; Chen, X. L.; Yu, R.; Lu, C. Z. Experimental and theoretical studies of highly emissive dinuclear Cu(I) halide complexes with delayed fluorescence. *Dalton Trans.* **2015**, 44, 11649–11659.
- (20) Huang, C. H.; Wen, M.; Wang, C. Y.; Lu, Y. F.; Huang, X. H.; Li, H. H.; Wu, S. T.; Zhuang, N. F.; Hu, X. L. A series of pure-blue-light emitting Cu(I) complexes with thermally activated delayed fluorescence: structural, photophysical, and computational studies. *Dalton Trans.* **2017**, 46, 1413–1419.
- (21) Linfoot, C. L.; Leidl, M. J.; Richardson, P.; Rausch, A. F.; Chepelin, O.; White, F. J.; Yersin, H.; Robertson, N. Thermally activated delayed fluorescence (TADF) and enhancing photoluminescence quantum yields of [CuI(diimine)(diphosphine)]⁺ complexes-photophysical, structural, and computational studies. *Inorg. Chem.* **2014**, 53, 10854–10861.
- (22) Nitsch, J.; Lacemon, F.; Lorbach, A.; Eichhorn, A.; Cisnetti, F.; Steffen, A. Cuprophilic interactions in highly luminescent dicopper(I)-NHC-picoly complexes-fast phosphorescence or TADF? *Chem. Commun.* **2016**, 52, 2932–2935.
- (23) Czerwieniec, R.; Leidl, M. J.; Homeier, H. H. H.; Yersin, H. Cu(I) complexes-thermally activated delayed fluorescence. Photophysical approach and material design. *Coord. Chem. Rev.* **2016**, 325, 2–28.